



HEAD AND NECK SQUAMOCELLULAR CARCINOMA: ADDED ROLE OF DIFFUSION WEIGHTED IMAGING

M. PICCOLI¹, S. PALMUCCI¹, F. ROCCASALVA¹, R. TAIBI², G.C. ETTORE²

¹Radiodiagnostic and Radiotherapy Unit, University Hospital "Policlinico-Vittorio Emanuele", Catania, Italy.

²Department of Medical Oncology, National Cancer Institute Aviano (PN), Italy.

Abstract: *Diffusion Weighted Imaging (DWI) represents a recent added value to conventional MRI. It is applied in many oncological diseases, improving detection of lesions and possibility of tissue characterization. Quantitative measurement – obtained calculating the Apparent Diffusion Coefficient (ADC) – has been proposed to better characterize the vitality of the oncological tissue. Head and Neck Squamous Cell Carcinoma (HNSCC) are predominantly diagnosed in advanced stage; subsequently, radiotherapy and chemotherapy are generally adopted at the beginning of treatment to reduce stage of disease. The changes in a tumour lesion are not easily assessed by conventional approaches, which are currently based on morphological features. Therefore, the role of diffusion MRI in the management of head and neck cancer has been proposed to early identify response to treatment. In addition, DWI capability in the assessment of nodal involvement and in the evaluation of residual/recurrence of disease after therapy is briefly discussed, explaining advantages due to its application in the management of HNSCC.*

KEY WORDS: *Diffusion magnetic resonance imaging, Magnetic resonance imaging, Head and neck neoplasms, Oropharyngeal neoplasms, Radiotherapy.*

INTRODUCTION

Squamous cell carcinomas are the most common type of malignant lesions that occur in the head and neck region, involving paranasal sinuses, nasal and oral cavities, pharynx and larynx^{1,2}. The incidence of Head and Neck Squamous Cell Carcinomas (HNSCC) is rising and currently is about 4-6% of all malignancies, with 650,000 new cases annually. The estimated yearly worldwide incidence is about half a million people, and nearly 50% of patients die of tumor-related complications³⁻⁵. A very high mortality of about 65000 deaths has been reported in European Countries^{3,6}.

HNSCC are most commonly encountered in men (M:F=5:1). Mainly, patients are affected during middle age (50-60 years)^{2,7}.

The most common HNSCC is laryngeal carcinoma. In males, squamous cell carcinomas of the larynx, oro- and hypopharynx are predominant, while in females, HNSCC are located mainly in the oral cavity and the oropharynx².

The predominant risk factors are tobacco and alcohol abuse, implicated in 75% of all neoplasms of this region; a strong connection with tobacco use has been reported⁸. HNSCC are usually sporadic, but the risk increases in patients with cancer susceptibility syndromes, such as hereditary non-polyposis colorectal cancer, Li-Fraumeni syndrome, Fanconi's anaemia, and ataxia telangiectasia¹.

Recently, many papers have investigated the role of human papillomavirus (HPV), mainly type 16, in the development of carcinomas of the oral cavity and the pharynx, especially the nasopharynx.



geal cancer, which is very rare in Europe⁹⁻¹². HPV positivity is considered an important factor in prevention, treatment and prognosis of these lesions. Therefore, HPV-related HNSCC seem to be more responsive to radiation, chemotherapy and immune surveillance of tumour-specific antigens^{10,13}.

Tumors located in the floor of the mouth and the oropharynx can usually be diagnosed clinically and endoscopically because of their superficial position².

An invasive cancer can grow in apparently healthy mucosa or on the site of a known precancerous lesion. In fact chronic inflammation of the oral mucosa, induced by tobacco, alcohol and other risk factors, leads to the development of precancerous lesions, such as leukoplakia and erythroplakia, that can be clinically detected¹.

Symptoms and signs of HNSCC are hoarseness, sore throat, tongue pain, otalgia, dysphagia and odynophagia, cough, mouth ulcer and bleeding. At clinical examination, the lesions generally appear as irregular vegetation or deep ulceration in oral cavity or oropharynx, while tumor could be found as a neck mass¹. Distant metastases are usually found in lung, mediastinum lymph nodes, liver and bones. The 5-year overall survival rate is usually less than 50%, although recent better tumour detection and multi-modal treatment for these lesions should lead to an improvement^{2,14}. Patients' prognosis is undoubtedly affected by delayed diagnosis, and unfortunately, more than 50% (about two-thirds) of patients show advanced stage disease at the onset². In addition, about 10% of patients have distant metastasis at initial presentation^{1,2}.

Close post-therapeutic patient monitoring, in the first two years after diagnosis of HNSCC, is essential for identifying and rapidly treating potential tumour recurrence, in order to improve patient outcome². Treatment consists of surgery combined with chemoradiotherapy. An appropriate disease management needs to consider some elements, such as primary tumour site, stage, possibility of resection, airway involvement and co-morbid illnesses¹.

Functional imaging has been recently applied in staging HNSCC. In fact, several papers have emphasized the contribution of perfusion CT, diffusion MRI, perfusion MRI and PET-CT in the evaluation of disease¹⁵⁻¹⁸. The main purpose of these modalities is to better characterize the vitality of the oncological tissue.

Therefore, this mini-review article has focused upon the role of diffusion MRI in the management of HNSCC, considering three main topics: 1) the contribution of Diffusion-Weighted Imaging (DWI) in monitoring response to treatment; 2) the role of DWI in the assessment of nodal involvement; 3) the possibility of diffusion MRI in the

evaluation of residual/recurrence of disease after therapy. Basic principles of DWI sequences are briefly discussed, in order to help clinicians, radiotherapists, surgeons and oncologists in their application in the management of HNSCC.

HNSCC Diagnosis: conventional and functional imaging

A biopsy of suspected malignant lesions is always needed to confirm the diagnosis, as the ease of access to sites of disease allows for many histological samples. After clinical inspection and endoscopic exams, conventional imaging with CT and MRI is generally performed to determine the stage of disease. These imaging modalities are essentially based on the morphological appearance of tissue, where tumor disease is detected for a different signal intensity or enhancement pattern in comparison with normal anatomical sites. Conventional imaging shows the extension of disease. However, the changes in a tumour lesion could not be easily assessed by conventional approaches, which are predominantly based on morphological features and two-dimensional measurements of tissue. In addition, they do not provide metabolic information about tissue.

PET/CT has been routinely added in the management of squamous cell cancer, because it provides metabolic information of tissues. PET/CT has been retained by many Authors to be superior to both CT and MRI in the detection of carcinoma of unknown primary, cervical nodes, distant metastasis, residual tumour and recurrent disease^{16,19-22}.

Recently, DWI has been widely introduced into many clinical fields, including oncological and non-oncological diseases. In literature, it has been applied in the assessment of fibrosis in chronic hepatic disease^{23,24}, in the detection of focal liver lesions^{25,26}. Diffusion MRI has also been used to evaluate the functionality of transplanted kidneys^{27,28}, the lesions' response in oncological patients^{29,30} and the assessment of tumour extent for gynaecological malignancies³¹. Recent studies have indicated DWI as a potential predictor biomarker³², which investigates the density of cellular population in a tissue and its change during treatment³³.

DWI: basic and principles

DWI provides measurement of free water motion in a tissue. Its sequence is based on a spin-echo sequence where re-focalization impulse is preceded and followed by an additional couple of pulses gradients³⁴⁻³⁶. These additional gradients have the same

intensity but opposite direction. Normally, free-circulating water molecules are exposed to the first gradient pulse, but phase shift due to first gradient is nullified by Brownian motion. The phase shift gained is generally equal to zero when molecules are free to diffuse in a “non-restricted” space. In some pathological conditions, such as neoplasms, ischemia, fibrosis or oedema, the intercellular spaces reduce their width and water molecules are restricted in movement. These restricted molecules are exposed to the first gradient, and do not have significant phase shift for movement. Subsequently, the second gradient is able to obtain re-focalization of the molecules; the signal intensity is a clear expression of restricted ambient.

The mentioned diffusion of water molecules in tissues (Brownian movement) is quantified by the ADC, which is calculated according to the following formula:

$$ADC = \ln(S_0/S_1)/b,$$

where S_0 is the signal intensity with $b=0$, S_1 is the signal intensity after the application of a given b gradient, and b is the value of the applied gradient³⁷.

Tissues with increased diffusivity generally have higher ADC values, whereas tissues with restricted diffusivity produce low ADC values (Figure 1).

Solid cancer shows high cellularity that concurs to restricted diffusion and lower ADC values (Figures 2 and 3)³⁸. However, subsequent cancer treatment induces cell death, increasing water diffusion and leading to a rise in ADC values. The good response after treatment associated with a reduction of cell population density should be indicated by changes in ADC values.

DWI in monitoring response to treatment

Chemoradiotherapy (CRT) is considered the standard treatment for patients with non-resectable HNSCC. This therapy preserves important func-

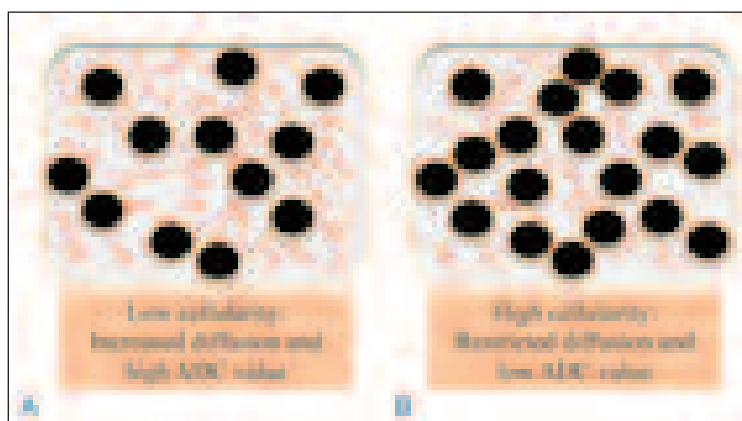
tionalties of head and neck districts (swallowing and speeches) and improves survival rate³⁹. However, since not all patients respond to therapy, it is important to find prognostic imaging biomarkers in order to predict early treatment outcomes.

These imaging biomarkers could stratify patients, distinguishing responders from non-responders at the time of pre- and early-treatment. The early detection of non-responders allows for the changing of therapeutic strategies, avoiding unnecessary toxicity and other negative side effects, which might increase long-term survival and quality of life^{39,40}.

The DWI potential in monitoring disease for head and neck was initially investigated in animal models with HNSCC. In the study by Hamstra et al⁴¹, diffusion MRI was performed in a population of orthotopic mouse model of SCCHN. Mice with murine squamous cells expressing the yeast transgene cytosine deaminase were treated with 5-fluorocytosine (5FC), radiotherapy, and combined therapy. They were compared with control animals for volumetric growth rate, diffusion, and survival. Mice treated with combined modality (ionizing radiation and chemotherapy) showed an increase in tumour diffusion values. This increase correlates with better survival⁴¹. Radiation therapy only had minimal effect on volumetric growth rate, diffusion and survival⁴¹. Therefore, the tumour diffusion change has a potential role as a clinical biomarker.

In another paper published by Galban et al⁴², primary HNSCC and cervical node metastases were studied in 15 patients before, during (3 weeks) and 6 months after treatment. ADC values were plotted in a histogram and the mean value was used to evaluate changes. The Authors showed that major ADC variation occurred in the complete responder group. They also introduced a PRM (Parametric Response Map) using a voxel-by-voxel analyses approach. This map consists of a voxel-to-voxel ADC change measurement. Changes in tumour cellular structures after CRT cause variations in ADC values, which are encoded as colour maps and overlaid on the

Fig. 1. ADC and different degrees of cellularity. Difference in ADC values is explained by the different degree of cellularity and water proton movements. Hypocellular tissues have large extracellular and intracellular spaces, with increased diffusion and high ADC value. Hypercellularity reduces extracellular spaces, which mean restricted diffusion and low signal on ADC map. Tumor after therapy changes its ADC value, because necrosis reduce cellularity, with consequent increasing of ADC values.



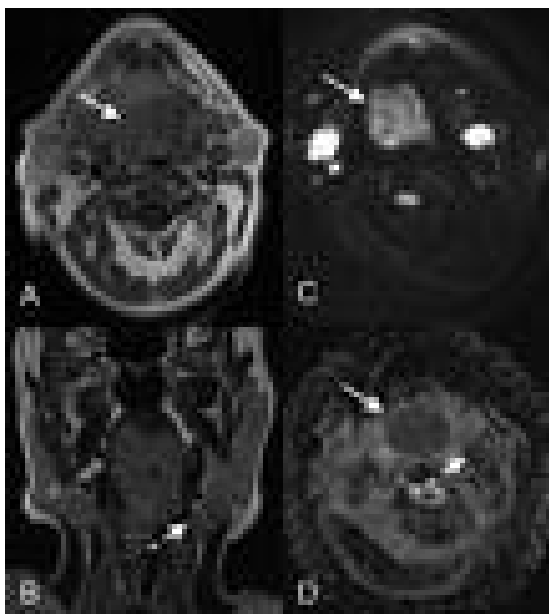


Fig. 2. Oropharyngeal cancer (centered on the base of the tongue, white arrows) and ADC map. Conventional MRI sequences (T1 and T2 weighted images, respectively A and B), diffusion image (C) and ADC map (D). Hypercellularity of the lesion means low signal on ADC map. Also nodes (dashed arrows) are clearly depicted (B and D).

MRI: “red” indicates increased ADC values, “blue” decreased ADC values and “green” unchanged ADC values^{17,42-43}. Following this colorimetric representation, the complete responder patients had a significantly high number of voxel with a significant increase in ADC values after therapy.

In the previous study, a significant correlation with outcomes has been demonstrated for changes in PRM and percentage change of tumor volume between baseline MRI and mid-therapy MRI observation. Percentage changes in mean ADC did not show any correlation with tumor control at 6 months^{17,42}.

However, early ADC changes could be more significant than tumor size changes, which normally

may be not observed. The early response to treatment and its role as early clinical biomarker was also confirmed by Kim et al⁴⁴. These Authors analysed ADC values in 33 patients with HNSCC and metastatic lymph nodes before, 1 week after beginning of therapy and post-treatment⁴⁴. They observed a significantly higher increase in ADC in the complete responder group at 1 week and after treatment. The ADC changes were due to necrosis induced by treatment and subsequently hypocellularity⁴⁴.

Response to treatment may have a different pattern of ADC changes. In fact, in a different study, King et al performed DWI in 50 patients affected by HNSCC³⁸. Quantitative assessment with ADC calculation was performed before and during therapy. The Authors described 4 different patterns: pattern A and B showed a continuous increase in ADC during treatment; an initial increase followed by a drop in ADC was described in pattern C; “an early fall followed by a late rise in ADC” in cases of pattern D³⁸.

Pattern A and B were considered more likely to have tumour control, while in pattern C and D, ADC drop was correlated with loco-regional failure, probably due to a regrowth of the lesion or tumour resistance. As reported by Authors, analysing serial changes (pre-, intra- and post-treatment) “a fall in ADC early or late in treatment has a high positive predictive value (100%) for loco regional failure”³⁸. A residual mass “without a drop in ADC was unlikely to have loco-regional failure in the first 6 months”³⁸. However, this does not exclude the possibility of late loco-regional disease growth^{38,39}.

According to results reported in the mentioned studies, baseline ADC values and ADC changes during treatment could be used as clinical biomarkers of response prediction.

A recent study directed by Chawla et al⁴⁵ suggested evaluation of both primary lesion and nodal masses in predicting treatment outcomes, using not only diffusion MRI but also perfusion parameters after contrast administration. They observed that the

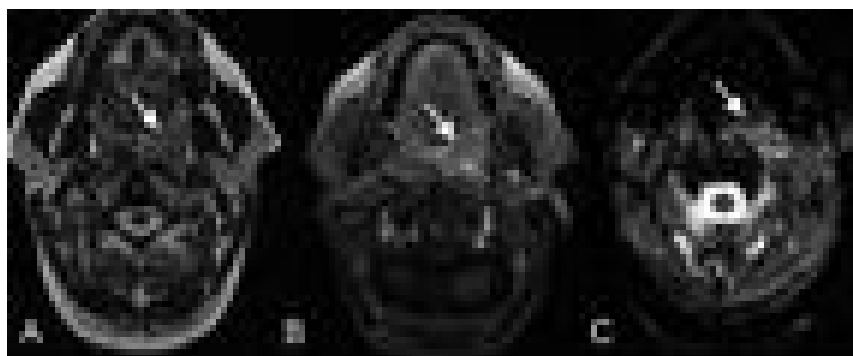


Fig. 3. Left tonsil tumor. Conventional MRI (T2 weighted and enhanced T1 acquisitions, respectively A and B), and ADC map (C). Tumor (white arrows) has low signal on ADC map.

heterogeneous nature of HNSCC influences the clinical course of the disease⁴⁶. Dynamic Contrast Enhanced (DCE) T1-weighted sequences were performed in a study by Cao et al¹⁸, in order to investigate response to therapy. The Authors found significantly increased blood volume (in the primary lesions) after 2 weeks of CRT in patients who had local disease control (at a median of 10 months), compared to subjects with local or regional failure. In this study what was very remarkable was that after 2 weeks, tumor volume reduction was not able to predict local disease control^{17,18}.

In another study, perfusion parameters were also investigated in a pre-treatment phase. The role of average contrast transfer coefficient (K^{trans}) was assessed, and it was significantly higher in complete responders than in those of non-responders. The DCE-MRI perfusion parameter K^{trans} reflected data of tumor blood flow and microvascular permeability. Elevated pre-treatment blood flow, blood volume and hypoxia showed high K values, and were correlated with greater response to CRT and prolonged survival⁴⁷. Although the findings of this study are very promising, they need confirmation from studies with a larger cohort of patients. The use of both DCE-MRI and PET represents a promising diagnostic tool for the better management of HNSCC. This combination reflects vascular and metabolic characteristics of neoplastic lesions⁴⁸.

DWI in the assessment of nodal involvement

Detection and characterization of lymph nodes represent crucial steps in the assessment of HNSCC. It has been widely reported that nodal metastasis are an adverse prognostic factor influencing outcome^{39,49}.

On routine imaging techniques, mainly CT and ultrasonography, the common criteria for differentiating metastatic from reactive lymph nodes are size (malignant lesions generally exceed >10 mm in short-axis diameter) and morphology. Metastatic lymph nodes generally appear irregular in shape, with ill-defined margins, abnormal internal architecture and central necrotic area^{49,50}. These morphological and dimensional criteria are not specific, because micro metastases could be found in normal size lymph nodes. Enlarged lymph nodes could be reactive³⁹, and do not contain malignant cells.

Functional MRI has recently been tested in the characterization of metastatic lymph nodes⁴⁹⁻⁵³. DWI plays an important role in the differentiation of metastatic from reactive lymph nodes, due to the different degree of cellularity⁴⁹. The role of DWI in

nodal staging and its impact on radiotherapy was evaluated in 22 patients with locally advanced HNSCC. Patients were studied with contrast-enhanced CT and MRI (including conventional sequences and DWI sequences). Target volumes for RT were assessed using a set of conventional sequences, another set of diffusion MR sequences, and finally a set based on pathology results. Diffusion MRI reported a sensitivity of 89% and a specificity of 97%; the higher agreement between imaging and pathology was found for DWI ($\kappa=0.97$) rather than for conventional imaging ($\kappa=0.56$)⁵¹. The difference between RT volumes and those obtained by pathology was calculated, and larger results were observed for conventional imaging, whereas DWI was more accurate in the identification of nodal gross tumor volume and nodal clinical target volume⁵¹. Based on results published by Dirx et al⁵¹, DWI is more accurate than conventional imaging for pre-radiotherapy nodal staging.

A quantitative approach calculating the ADC map was suggested for differentiating benign from malignant nodes⁵³. In a recent study by Vandecaveye et al⁵³, a comparison between conventional TSE T2-weighted images and DWI sequences was performed. The Authors calculated the ADC of lymph nodes of 4 mm or greater in short axis diameter. Nodes were subsequently evaluated microscopically using prekeratin immunostaining. Radiological-pathological correlation was obtained for a total of 301 nodes. The mean ADC values for benign nodes was $1.19 \times 10^{-3} \text{ mm}^2/\text{sec}$, whereas for malignant ones a mean ADC value of $0.85 \times 10^{-3} \text{ mm}^2/\text{sec}$ was reported. Using a threshold of $0.9485 \times 10^{-3} \text{ mm}^2/\text{sec}$, the study reported sensitivity, specificity and accuracy respectively of 84%, 94% and 91% for differentiation of malignant from benign nodes; “for differentiation at each level”, sensitivity, specificity and accuracy were respectively 94%, 94% and 97%⁵³. Comparing with conventional TSE sequences, DWI reported higher sensitivity (76% versus 7%), but “slightly lower specificity” (94% versus 99.5%)⁵³. This study suggests that the use of DWI together with standard criteria of size and morphology, helps radiologists in the discrimination of lymph nodes and decrease false-positive data⁵³.

According to results published in literature, metastatic lymph nodes have a significantly low signal on ADC map compared with benign reactive and granulomatous lymph nodes. A low ADC value is also typical of lymphoma, but in this case, it is lower than in metastatic lymph nodes⁴³. The difference in water proton diffusion is due to various degrees of cellularity, necrosis and perfusion. Hypercellularity, large areas of necrosis and hypervascularization of head and neck squamous cell carcinoma influence



the restriction of diffusion, reflecting the low ADC value⁵². Sometimes, the difference between small areas of metastatic deposits and foci of necrosis is difficult to evaluate. Therefore, DWI should be combined with TSE MR sequences⁵³. However, a quantitative approach of adopting a threshold level of ADC is limited by a certain degree of overlap between malignant and benign nodes.

Evaluation of residual/recurrence of disease after therapy

HNSCC treatment consists of surgery, radiotherapy and chemotherapy⁵¹. These therapies induce some variations in tissues, such as oedema, inflammatory and fibrous reaction, scarring of nearby tissue and perichondritis^{37,54-56}.

A recurrent question for clinicians and radiologists regards the differentiation between post-therapeutic changes and a residual or recurrence of neoplastic disease. Unfortunately, using routine imaging tools, it is very difficult to differentiate residual/recurrence disease from post-treatment changes, because imaging findings are similar^{37,38,54}.

Several studies have already demonstrated that PET-CT has higher diagnostic accuracy than conventional imaging modalities in the evaluation of tumor response and in the characterization of residual neoplastic disease^{16,57,58}. Sensitivity, specificity, PPV and NPV for residual primary tumor after treatment were respectively 94%, 82%, 75% and 95%^{16,59}. In assessing residual disease, high NPV and specificity of the neck after chemoradiotherapy have been documented. In patients without residual lymphadenopathy at PET-CT, neck dissection could be safely performed. However, PPV is considered “suboptimal⁵⁹: further studies are needed in order to confirm the role of PET-CT⁶⁰”.

A promising tool could be the diffusion of MRI and ADC values, which allow for the differentiation between residual or recurrence tumour after therapy⁶¹. In particular, quantitative and qualitative evaluation is required, including, subsequently, the relative ADC map.

Recurrence or residual tumors show hyper-intense signal in images with high b-value, with low signal on ADC map. Post-therapeutic changes, instead, have a variable signal in image with high b-value, but quantitative assessment using ADC map show high signal³⁷.

This difference in ADC values is explained by the different degree of cellularity and water proton movements. Tumors are hyper-cellular, and the water diffusion in extracellular and intracellular spaces is reduced, with low signal on ADC map. In post-therapeutic phase, instead, the tissue is hypo-

cellular and oedema with inflammatory changes increases the diffusion of water proton, with high signal on ADC map^{54,61}.

Conclusions

Recent advances in MRI allow for better characterization of oncological neck diseases, adding – to morphological assessment – functional evaluation using diffusion sequences. DWI investigates the cellularity of oncological tissue and its change during therapy. Pre-treatment ADC value represents a diagnostic tool for predicting response to therapy; moreover, ADC changes during therapy could be used for monitoring response to treatment. Prospective studies are needed to better define the functional role of MRI in the evaluation of HNSCC: an intermediate diffusion MRI during treatment could be performed in order to early identify responders and non-responders patients.

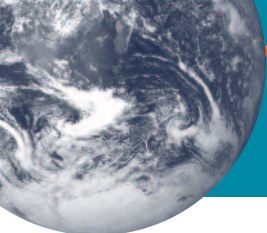
Conflict of Interests:

The Authors declare that they have no conflict of interests.

References

1. ARGIRIS A, KARAMOUZIS MV, RABEN D, FERRIS RL. Head and neck cancer. *Lancet* 2008; 371: 1695-1709.
2. SADICK M, SCHOENBERG SO, HOERMANN K, SADICK H. Current oncologic concepts and emerging techniques for imaging of head and neck squamous cell cancer. *GMS Curr Top Otorhinolaryngol Head Neck Surg* 2012; 11: Doc08.
3. WIKNER, GRÖBE A, PANTEL K, RIETHDORF S. Squamous cell carcinoma of the oral cavity and circulating tumour cells. *World J Clin Oncol* 2014; 5: 114-124.
4. PARKIN DM, BRAY F, FERLAY J, PISANI P. Estimating the world cancer burden: Globocan 2000. *Int J Cancer* 2001; 94: 153-156.
5. HADDAD RI, SHIN DM. Recent advances in head and neck cancer. *N Engl J Med* 2008; 359: 1143-1154.
6. BARNES L. World health organisation classification of tumours, pathology and genetics, head and neck tumours. Lyon: IARC Press, 2005
7. BRAAKHUIS BJ, LEEMANS CR, VISSER O. Incidence and survival trends of head and neck squamous cell carcinoma in the Netherlands between 1989 and 2011. *Oral Oncol* 2014; 50: 670-675.
8. VIGNESWARAN N, WILLIAMS MD. Epidemiological Trends in Head and Neck Cancer and Aids in Diagnosis. *Oral Maxillofac Surg Clin North Am* 2014; 26: 123-141.
9. MATSUMOTO F, FUJIMAKI M, OHBA S, KOJIMA M, YOKOYAMA J, IKEDA K. Relation between insulin-like growth factor-1 receptor and human papilloma virus in patients with oropharyngeal cancer. *Head Neck* 2014 Apr 2. doi: 10.1002/hed.23702 [Epub ahead of print]
10. NICHOLS AC, FINKELSTEIN DM, FAQUIN WC, WESTRA WH, MROZ EA, KNEUERTZ P, BEGUM S, MICHAUD WA, BUSSE PM, CLARK JR, ROCCO JW. Bcl2 and human papilloma virus 16 as predictors of outcome following concurrent chemoradiation for advanced oropharyngeal cancer. *Clin Cancer Res* 2010; 16: 2138-2146.

11. IHLOFF AS, PETERSEN C, HOFFMANN M, KNECHT R, TRIBIUS S. Human papilloma virus in locally advanced stage III/IV squamous cell cancer of the oropharynx and impact on choice of therapy. *Oral Oncol* 2010; 46: 705-711.
12. MORBINI P, DAL BELLO B, ALBERIZZI P, MANNARINI L, MEVIO N, GAROTTA M, MURA F, TINELLI C, BERTINO G, BENAZZO M. Oral HPV infection and persistence in patients with head and neck cancer. *Oral Surg Oral Med Oral Pathol Oral Radiol* 2013; 116: 474-84.
13. LICITRA L, PERRONE F, BOSSI P, SUARDI S, MARIANI L, ARTUSI R, OGGIONI M, ROSSINI C, CANTÙ G, SQUADRELLI M, QUATRONE P, LOCATI LD, BERGAMINI C, OLMI P, PIEROTTI MA, PILOTTI S. High-risk human papillomavirus affects prognosis in patients with surgically treated oropharyngeal squamous cell carcinoma. *J Clin Oncol* 2006; 24: 5630-5636.
14. GUNTINAS-LICHIUS O, WENDT T, BUENTZEL J, ESSER D, LOCHNER P, MUELLER A, SCHULTZE-MOSGAU S, ALTENDORF-HOFMANN A. Head and neck cancer in Germany: a site-specific analysis of survival of the Thuringian cancer registration database. *J Cancer Res Clin Oncol* 2010; 136: 55-63.
15. EMONTS P, BOURGEOIS P, LEMORT M, FLAMEN P. Functional imaging of head and neck cancers. *Curr Opin Oncol* 2009; 21: 212-217.
16. TANTIWONGKOSI B, YU F, KANARD A, MILLER FR. Role of 18F-FDG PET/CT in pre and post treatment evaluation in head and neck carcinoma. *World J Radiol* 2014; 6: 177-191.
17. SRINIVASAN A, MOHAN S, MUKHERJI SK. Biologic imaging of head and neck cancer: the present and the future. *AJNR Am J Neuroradiol* 2012; 33: 586-594.
18. CAO Y, POPOVTZER A, LI D, CHEPEHA DB, MOYER JS, PRINCE ME, WORDEN F, TEKNOS T, BRADFORD C, MUKHERJI SK, EISBRUCH A. Early prediction of outcome in advanced headand-neck cancer based on tumor blood volume alterations during therapy: a prospective study. *Int J Radiat Oncol Biol Phys* 2008; 72: 1287-1290.
19. HA PK, HDEIB A, GOLDENBERG D, JACENE H, PATEL P, KOCH W, CALIFANO J, CUMMINGS CW, FLINT PW, WAHL R, TUFANO RP. The role of positron emission tomography and computed tomography fusion in the management of early-stage and advanced-stage primary head and neck squamous cell carcinoma. *Arch Otolaryngol Head Neck Surg* 2006; 132: 12-16.
20. MILLER FR, HUSSEY D, BEERAM M, ENG T, MCGUFF HS, OTTO RA. Positron emission tomography in the management of unknown primary head and neck carcinoma. *Arch Otolaryngol Head Neck Surg* 2005; 131: 626-629.
21. GUPTA T, MASTER Z, KANNAN S, AGARWAL JP, GHOSH-LASKAR S, RANGARAJAN V, MURTHY V, BUDRUKAR A. Diagnostic performance of post-treatment FDG PET or FDG PET/CT imaging in head and neck cancer: a systematic review and meta-analysis. *Eur J Nucl Med Mol Imaging* 2011; 38: 2083-2095.
22. SCOTT AM, GUNAWARDANA DH, BARTHOLOMEUSZ D, RAMSHAW JE, LIN P. PET changes management and improves prognostic stratification in patients with head and neck cancer: results of a multicenter prospective study. *J Nucl Med* 2008; 49: 1593-1600.
23. TAOULI B, CHOULI M, MARTIN AJ, QAYYUM A, COAKLEY FV, VILGRAIN V. Chronic hepatitis: role of diffusion-weighted imaging and diffusion tensor imaging for the diagnosis of liver fibrosis and inflammation. *J Magn Reson Imaging* 2008; 28: 89-95.
24. PASQUINELLI F, BELLI G, MAZZONI LN, REGINI F, NARDI C, GRAZIOLI L, ZIGNEGO AL, COLAGRANDE S. MR-diffusion imaging in assessing chronic liver diseases: does a clinical role exist? *Radiol Med* 2012; 117: 242-253.
25. PALMUCCI S, MAURO LA, MESSINA M, RUSSO B, FAILLA G, MILONE P, BERRETTA M, ETTORE GC. Diffusion-weighted MRI in a liver protocol: its role in focal lesion detection. *World J Radiol* 2012; 4: 302-310.
26. BRUGGE M, HOLZAPPEL K, GAA J, WOERTLER K, WALDT S, KIEFER B, STEMMER A, GANTER C, RUMMENY EJ. Characterization of focal liver lesions by ADC measurements using a respiratory triggered diffusion-weighted single-shot echo-planar MR imaging technique. *Eur Radiol* 2008; 18: 477-485.
27. PALMUCCI S, MAURO LA, VEROUX P, FAILLA G, MILONE P, ETTORE GC, SINAGRA N, GIUFFRIDA G, ZERBO D, VEROUX M. Magnetic resonance with diffusion-weighted imaging in the evaluation of transplanted kidneys: preliminary findings. *Transplant Proc* 2011; 43: 960-966.
28. PALMUCCI S, MAURO LA, FAILLA G, FOTI PV, MILONE P, SINAGRA N, ZERBO D, VEROUX P, ETTORE GC, VEROUX M. Magnetic resonance with diffusion-weighted imaging in the evaluation of transplanted kidneys: updating results in 35 patients. *Transplant Proc* 2012; 44: 1884-1888.
29. MUNGAI F, PASQUINELLI F, MAZZONI LN, VIRGILI G, RAGOZZINO A, QUAIA E, MORANA G, GIOVAGNONI A, GRAZIOLI L, COLAGRANDE S. Diffusion-weighted magnetic resonance imaging in the prediction and assessment of chemotherapy outcome in liver metastases. *Radiol Med* 2014; 119: 625-633.
30. KOKABI N, CAMACHO JC, XING M, QIU D, KITAJIMA H, MITTAL PK, KIM HS. Apparent diffusion coefficient quantification as an early imaging biomarker of response and predictor of survival following yttrium-90 radioembolization for unresectable infiltrative hepatocellular carcinoma with portal vein thrombosis. *Abdom Imaging* 2014; 39: 969-978.
31. LEVY A, MEDJHOUL A, CARAMELLA C, ZARESKI E, BERGES O, CHARGARI C, BOULET B, BIDAULT F, DROMAIN C, BALLEYGUIER C. Interest of diffusion-weighted echo-planar MR imaging and apparent diffusion coefficient mapping in gynecological malignancies: a review. *J Magn Reson Imaging* 2011; 33: 1020-1027.
32. FARJAM R, TSIEN CI, FENG FY, HAYMAN JA, LAWRENCE TS, CAO Y. Diffusion abnormality index: a new imaging biomarker for early assessment of tumor response to therapy. *Pract Radiat Oncol* 2013; 3(2 Suppl 1): S5.
33. MOFFAT BA, CHENEVERT TL, LAWRENCE TS, MEYER CR, JOHNSON TD, DONG Q, TSIEN C, MUKHERJI S, QUINT DJ, GEBARSKI SS, ROBERTSON PL, JUNCK LR, REHEMTULLA A, ROSS BD. Functional diffusion map: a noninvasive MRI biomarker for early stratification of clinical brain tumor response. *Proc Natl Acad Sci USA* 2005; 102: 5524-5529.
34. LE BIHAN D, TURNER R, PEKAR J, MOONEN CTW. Diffusion and perfusion imaging by gradient sensitization: design, strategy and significance. *J Magn Reson Imaging* 1991; 1: 7-28.
35. LE BIHAN D. Molecular diffusion nuclear magnetic resonance imaging. *Magn Reson Q* 1991; 7: 1-28.
36. TURNER R, LE BIHAN D, CHESNICK AS. Echo-planar imaging of diffusion and perfusion. *Magn Reson Med* 1991; 19: 247-253.
37. COLAGRANDE S, CARBONE SF, CARUSI LM, COVA M, VILLARI N. Magnetic resonance diffusion-weighted imaging: extra-neurological applications. *Radiol Med* 2006; 111: 392-419.
38. KING AD, Mo FK, YU KH, YEUNG DK, ZHOU H, BHATIA KS, TSE GM, VLANTIS AC, WONG JK, AHUJA AT. Squamous cell carcinoma of the head and neck: diffusion-weighted MR imaging for prediction and monitoring of treatment response. *Eur Radiol* 2010; 20: 2213-2220.
39. THOENY HC. Diffusion-weighted MRI in head and neck radiology: applications in oncology. *Cancer Imaging* 2011; 10: 209-214.
40. LEE J, MOON C. Current status of experimental therapeutics for head and neck cancer. *Exp Biol Med (Maywood)* 2011; 236: 375-389.
41. HAMSTRA DA, LEE KC, MOFFAT BA, CHENEVERT TL, REHEMTULLA A, ROSS BD. Diffusion magnetic resonance imaging: an imaging treatment response biomarker to chemoradiotherapy in a mouse model of squamous cell cancer of the head and neck. *Transl Oncol* 2008; 1: 187-194.



42. GALBÁN CJ, MUKHERJI SK, CHENEVERT TL, MEYER CR, HAMSTRA DA, BLAND PH, JOHNSON TD, MOFFAT BA, REHEMTULLA A, EISBRUCH A, ROSS BD. A feasibility study of parametric response map analysis of diffusion-weighted magnetic resonance imaging scans of head and neck cancer patients for providing early detection of therapeutic efficacy. *Transl Oncol* 2009; 2: 184-90.
43. THOENY HC, ROSS BD. Predicting and monitoring cancer treatment response with diffusion-weighted MRI. *J Magn Reson Imaging* 2010; 32: 2-16.
44. KIM S, LOEVNER L, QUON H, SHERMAN E, WEINSTEIN G, KILGER A, POPTANI H. Diffusion-weighted magnetic resonance imaging for predicting and detecting early response to chemoradiation therapy of squamous cell carcinomas of the head and neck. *Clin Cancer Res* 2009; 15: 986-994.
45. CHAWLA S, KIM S, DOUGHERTY L, WANG S, LOEVNER LA, QUON H, POPTANI H. Pretreatment Diffusion-Weighted and Dynamic Contrast-Enhanced MRI for prediction of local treatment Response in Squamous Cell Carcinomas of the head and neck. *AJR Am J Roentgenol* 2013; 200: 35-43.
46. VENERONI S, SILVESTRINI R, COSTA A, SALVATORI P, FARANDA A, MOLINARI RL. Biological indicators of survival in patients treated by surgery for squamous cell carcinoma of the oral cavity and oropharynx. *Oral Oncol* 1997; 33: 408-413.
47. ZIMA A, CARLOS R, GANDHI D, CASE I, TEKNOS T, MUKHERJI SK. Can pretreatment CT perfusion predict response of advanced squamous cell carcinoma of the upper aerodigestive tract treated with induction chemotherapy? *AJNR Am J Neuroradiol* 2007; 28: 328-334.
48. CATANA C, PROCISSI D, WU Y, JUDENHOFER MS, QI J, PICHLER BJ, JACOBS RE, CHERRY SR. Simultaneous in vivo positron emission tomography and magnetic resonance imaging. *Proc Natl Acad Sci USA* 2008; 105: 3705-3710.
49. DE BONDT RBJ, HOEBERIGS MC, NELEMANS PJ, DESERNO WM, PEUTZ-KOOTSTRA C, KREMER B, BEETS-TAN RG. Diagnostic accuracy and additional value of diffusion-weighted imaging for discrimination of malignant cervical lymph nodes in head and neck squamous cell carcinoma. *Neuroradiology* 2009; 51: 183-192.
52. SUMI M, SAKIHAMA N, SUMI T, MORIKAWA M, UETANI M, KABASAWA H, SHIGENO K, HAYASHI K, TAKAHASHI H, NAKAMURA T. Discrimination of Metastatic Cervical Lymph Nodes with Diffusion-Weighted MR Imaging in Patients with Head and Neck Cancer. *Am J Neuroradiol* 2003; 24: 1627-1634.
53. DIRIX P, VANDECAVEYE V, DE KEYZER F, OP DE BEECK K, POORTEN VV, DELAERE P, VERBEKEN E, HERMANS R, NUYTS S. Diffusion-weighted MRI for nodal staging of head and neck squamous cell carcinoma: impact on radiotherapy planning. *Int J Radiat Oncol Biol Phys* 2010; 76: 761-766.
54. KING AD, AHUJA AT, YEUNG DK, FONG DK, LEE YY, LEI KI, TSE GM. Malignant cervical lymphadenopathy: diagnostic accuracy of diffusion-weighted MR imaging. *Radiology* 2007; 245: 806-813.
55. VANDECAVEYE V, DE KEYZER F, POORTEN VV, DIRIX P, VERBEKEN E, NUYTS S, HERMANS R. Head and neck squamous cell carcinoma: value of diffusion-weighted MR imaging for nodal staging. *Radiology* 2009; 251: 134-146.
56. ABDEL RAZEK AAK, KANDEEL AY, SOLIMAN N, EL-SHENS-HAWY HM, KAMEL Y, NADA N, DENEWAR A. Role of diffusion-weighted Echo-Planar MR Imaging in differentiation of residual or recurrent head and neck tumors and posttreatment changes. *Am J Neuroradiol* 2007; 28: 1146-1152.
57. TSHERING VOGEL DW, ZBAEREN P, THOENY HC. Cancer of the oral cavity and oropharynx. *Cancer Imaging* 2010; 10: 62-72.
58. TAIBI R, LLESHI A, BARZAN L, FIORICA F, LEGHISSA M, VACCHER E, DE PAOLI P, FRANCHIN G, BERRETTA M, TIRELLI U. Head and neck cancer survivors patients and late effects related to oncologic treatment: update of literature. *Eur Rev Med Pharmacol Sci* 2014; 18: 1473-1481.
59. BRONSTEIN AD, NYBERG DA, SCHWARTZ AN, SHUMAN WP, GRIFFIN BR. Soft-tissue changes after head and neck radiation: CT findings. *AJNR Am J Neuroradiol* 1989; 10: 171-175.
60. LAUBENBACHER C, SAUMWEBER D, WAGNER-MANSLAU C, KAU RJ, HERZ M, AVRIL N, ZIEGLER S, KRUSCHKE C, ARNOLD W, SCHWAIGER M. Comparison of fluorine-18-fluorodeoxyglucose PET, MRI and endoscopy for staging head and neck squamous-cell carcinomas. *J Nucl Med* 1995; 36: 1747-1757.
61. GUPTA T, MASTER Z, KANNAN S, AGARWAL JP, GHOSH-LASKAR S, RANGARAJAN V, MURTHY V, BUDRUKKAR A. Diagnostic performance of post-treatment FDG PET or FDG PET/CT imaging in head and neck cancer: a systematic review and meta-analysis. *Eur J Nucl Med Mol Imaging* 2011; 38: 2083-2095.
62. ONG SC, SCHÖDER H, LEE NY, PATEL SG, CARLSON D, FURY M, PFISTER DG, SHAH JP, LARSON SM, KRAUS DH. Clinical utility of 18F-FDG PET/CT in assessing the neck after concurrent chemoradiotherapy for Locoregional advanced head and neck cancer. *J Nucl Med* 2008; 49: 532-40.
63. HWANG I, CHOI SH, KIM YJ, KIM KG, LEE AL, YUN TJ, KIM JH, SOHN CH. Differentiation of recurrent tumor and post-treatment changes in head and neck squamous cell carcinoma: application of high b-value diffusion-weighted imaging. *AJNR Am J Neuroradiol* 2013; 34: 2343-2348.